

**STUDY ON SOLAR ULTRAVIOLET
ERYTHEMAL DOSE DISTRIBUTION
OBTAINED BY AURA SATELLITE OVER
PENINSULAR MALAYSIA**

NOR HIDAYAH BINTI HISAMUDDIN SHAH

UNIVERSITI SAINS MALAYSIA

2013

**STUDY ON SOLAR ULTRAVIOLET ERYTHEMAL DOSE
DISTRIBUTION OBTAINED BY AURA SATELLITE OVER
PENINSULAR MALAYSIA**

By

NOR HIDAYAH BINTI HISAMUDDIN SHAH

**Thesis submitted in fulfillment of requirements for
the degree of Master of Science**

June 2013

ACKNOWLEDGEMENT

I wish to express my thanks to my Main Supervisor Professor Mohd Zubir Bin Mat Jafri and my co-supervisor Dr. Lim Hwee San for their help and guidance throughout the course of my study. Their essential and constructive comments have enabled me to successfully complete this research thesis.

I would like to express my very great appreciation to Dr Jasim Rajab for his valuable and constructive suggestions during the planning and development of this research work. His willingness to give his time so generously has been very much appreciated. I also would like to gratefully acknowledge the help and support of all the Staff and researcher at the Engineering Physics Lab, USM. For access to the OMUVBd data, I wish to thank Dr. Antti Arola and Dr. Niilo Kalakoski from Finnish Meteorological Institute for guiding the usage of UV erythema dose data.

The experimental part of this research has been supported through an USM-PGRS funded. Lastly, my special thanks to my mother Ms. Naimah and my family for their patience, love, encouragement and emotional support throughout my study period. I regret only that my father, Mr. Hisamuddin Shah who gave me full support, self-belief and confidence are not around. I dedicate this work to him. Also to all my close friends, Nurul, Tengku Sarah, Aifa, Atika Atira, Waheeda, Yusbita, Sabihah, Suhana, Safra and Fara, I would like to thank them for their unstoppable loves and helps. I would have not finished this project without the support from them and they have always been there for me.

TABLE OF CONTENTS

ACKNOWLEDGEMENTS	ii
TABLE OF CONTENTS	iii
LIST OF TABLES	vi
LIST OF FIGURES	vii
LIST OF ABBREVIATIONS	x
ABSTRAK	xii
ABSTRACT	xiv
CHAPTER 1:	1
INTRODUCTION	
1.0 Introduction	1
1.1 Ultraviolet Radiation	3
1.2 Factors Affecting Ultraviolet Radiation	5
1.3 UV Index	9
1.4 Daily Ultraviolet Erythema Dose	10
1.5 Problem Statement	11
1.6 Objectives of the Study	12
1.7 Outline of the Thesis	13
CHAPTER 2:	14
LITERATURE REVIEW	
2.0 Introduction	14

2.1 AURA Satellite	14
2.1.1 Ozone Monitoring Instrument	15
2.1.2 UV Algorithm Overview	18
2.2 O3M SAF	19
2.2.1 Offline UV daily dose	19
2.3 Validation on OMI Data	21
CHAPTER 3:	25
METHODOLOGY	
3.0 Introduction	25
3.1 Remote Sensing Data Format	24
3.1.1 OMI UVB Level 3 HDF-EOS (OMUVBd)	25
3.1.2 O3M SAF Offline UV product (OUV)	26
3.2 Study Area and Period	27
3.3 Softwares	28
3.4 Procedures	29
CHAPTER 4:	32
RESULT AND DATA ANALYSIS	
4.0 Introduction	32
4.1 Monthly Mean Ultraviolet Erythemal Dose	
Distribution Maps for 2009	32
4.2 Daily Mean Ultraviolet Erythemal Dose for 2009	38

CHAPTER 5:	41
COMPARISON WITH O3M SAF DATA	
5.0 Introduction	41
5.1 Monthly Mean Absolute Difference Maps	41
5.2 Monthly Mean Relative Difference Maps	46
5.3 Discussion	50
CHAPTER 6:	56
CONCLUSIONS	
6.0 Overview	56
6.1 Conclusion	56
6.2 Further Study	57
REFERENCE	58
APPENDICES	66

LIST OF TABLE

Table 2.1	OMI instrument characteristic	17
Table 2.2	O3M SAF Product Tables for Offline UV daily	20
Table 3.1	Highest, lowest and monthly mean erythemal dose over Peninsular Malaysia on 2009	39

LIST OF FIGURES

Figure 1.1	Ultraviolet (UV) region of the electromagnetic spectrum	2
Figure 1.2	The annual mean global nergy budget for the earth-atmosphere system.	3
Figure 1.3	Long-term changes in surface erythemal radiation	8
Figure 1.4	UV dose in De Bilt on 1 June 2002	10
Figure 1.5	UV dose in Augsburg on 1 June	11
Figure 2.1	Measurement design of Ozone Monitoring Instrument	16
Figure 2.2	OMI UV algorithm overview	18
Figure 3.1	Study area: Peninsular Malaysia, starting from [0°N, 99°E] until [9°N, 106°E]	27
Figure 3.2	OMUVBd view using HDF Explorer	30
Figure 3.3	OUV view using HDF Explorer	31
Figure 4.1	Monthly Mean Erythemal Dose for January 2009	33
Figure 4.2	Monthly Mean Erythemal Dose for February 2009	33
Figure 4.3	Monthly Mean Erythemal Dose for March 2009	33
Figure 4.4	Monthly Mean Erythemal Dose for April 2009	34
Figure 4.5	Monthly Mean Erythemal Dose for May 2009	34
Figure 4.6	Monthly Mean Erythemal Dose for June 2009	34
Figure 4.7	Monthly Mean Erythemal Dose for July 2009	35

Figure 4.8	Monthly Mean Erythemal Dose for August 2009	35
Figure 4.9	Monthly Mean Erythemal Dose for September 2009	35
Figure 4.10	Monthly Mean Erythemal Dose for October 2009	36
Figure 4.11	Monthly Mean Erythemal Dose for November 2009	36
Figure 4.12	Monthly Mean Erythemal Dose for December 2009	36
Figure 4.13	Graph of daily distribution Ultraviolet erythemal dose for year 2009	39
Figure 4.14	Monthly mean of Ultraviolet erythemal dose for year 2009	39
Figure 5.1	Monthly mean absolute difference between OMUVB and OUV for June 2009	42
Figure 5.2	Monthly mean absolute difference between OMUVB and OUV for July 2009	42
Figure 5.3	Monthly mean absolute difference between OMUVB and OUV for August 2009	43
Figure 5.4	Monthly mean absolute difference between OMUVB and OUV for September 2009	43
Figure 5.5	Monthly mean absolute difference between OMUVB and OUV for October 2009	44
Figure 5.6	Monthly mean absolute difference between OMUVB and OUV for November 2009	44
Figure 5.7	Monthly mean absolute difference between OMUVB and OUV for December 2009.	45
Figure 5.8	Monthly mean relative difference between OMUVB and OUV for June 2009	47

Figure 5.9	Monthly mean relative difference between OMUVB and OUV for July 2009	47
Figure 5.10	Monthly mean relative difference between OMUVB and OUV for August 2009	48
Figure 5.11	Monthly mean relative difference between OMUVB and OUV for September 2009	48
Figure 5.12	Monthly mean relative difference between OMUVB and OUV for October 2009	49
Figure 5.13	Monthly mean relative difference between OMUVB and OUV for November 2009	49
Figure 5.14	Monthly mean relative difference between OMUVB and OUV for December 2009	50
Figure 5.15	Histogram of monthly absolute differences [(OMUVB-OUV)] for June 2009 until December 2009	51
Figure 5.16	Histogram of monthly mean relative differences [(OMUVB- OUV)/OUV] for June 2009 until December 2009	52
Figure 5.17	Correlation of Erythemal UV Dose from Ozone Monitoring Instrument with an Offline UV O3M SAF data near Penang.	53
Figure 5.18	Correlation of Erythemal UV Dose from Ozone Monitoring Instrument with an Offline UV O3M SAF data near Kuantan.	54

LIST OF ABBREVIATIONS

AVHRR	Advanced Very High Resolution Radiometer
BUV	Backscatter Ultraviolet
CCD	Charge-Coupled Device
CIE	Commission Internationale de l'Éclairage, International Commission on Illumination.
EOS	Earth Observing System
EUV	Erythemal Ultraviolet
EUMETSAT	European Organisation for the Exploitation of Meteorological Satellites
FMI	Finnish Meteorological Institute
FOV	Field of View
FWHM	Full Width at Half Maximum
GOME-2	Global Ozone Monitoring Experiment, version 2
HDF	Hierarchical Data Format
HDF-5	Hierarchical Data Format, current level HDF5
HDF-EOS EOS	The prescribed format for standard data products derived from EOS
HIRDLS	High Resolution Dynamics Limb Sounder
KNMI	The Royal Netherlands Meteorological Institute
LER	Lambertian-Equivalent Reflectivity
MLER	Mixed Lambertian-Equivalent Reflectivity
MLS	Microwave Limb Sounder
NIVR	The Netherlands Agency for Aerospace Programmes
O3M SAF	Satellite Application Facility on Ozone and Atmospheric Chemistry Monitoring
OMI	Ozone Monitoring Instrument
OMUVBd	Level-3 OMI Surface UV Irradiance and Erythemal Dose

OUV	Offline Ultraviolet Product
RAF	Radiation Amplification Factor
RMS	Root-Mean-Square (power measurement)
SBUV	Solar Backscatter Ultraviolet (instrument)
SCIAMACHY	Scanning Imaging Absorption Spectrometer for Atmospheric Cartography
SZA	Solar Zenith Angle
TES	Tropospheric Emission Spectrometer
TOMS	Total Ozone Mapping Spectrometer
UV	Ultra Violet
UVI	UV Aerosol Index
VIS	Visible

KAJIAN TABURAN DOS ERITERMA SINARAN ULTRAUNGU SURIA DI SEMENANJUNG MALAYSIA MENGGUNAKAN DATA SATELIT AURA

ABSTRAK

Sejak 30 tahun lepas, dos eriterma sinaran ultraungu (UV) dari matahari telah meningkat di kebanyakan tempat di seluruh dunia, terutamanya di negara pertengahan latitud. Maklumat mengenai jumlah dos eriterma yang sampai ke bumi adalah sangat penting untuk keselamatan manusia dan benda hidup yang lain. Untuk kajian ini, data satelit bernama 'Level-3 OMI Surface UV Irradiance and Erythemal Dose' (OMUVBd) yang diterima dari 'Ozone Monitoring Instrument' (OMI) yang dipasang di satelit bernama 'AURA' telah diambil untuk dikaji. Kajian mengenai dos eriterma ultraungu telah bermula pada 1 Januari 2009 hingga 31 Disember 2009. Tujuan tesis ini adalah untuk mengkaji taburan dos eriterma di Semenanjung Malaysia menggunakan data 'remote sensing' bernama OMUVBd mengikut bulan dan mengkaji perbezaan bacaan data OMUVBd dengan data satelit yang lain. Bacaan tertinggi dos eriterma ultraungu harian untuk semenanjung Malaysia direkodkan pada bulan March dengan bacaan purata 6330.78 J/m^2 yang mana pada ketika itu sudut zenith matahari menunjukkan bacaan sifar. Purata dos eriterma sepanjang tempoh kajian adalah 5447.33 J/m^2 . Bacaan purata terendah yang direkodkan adalah pada bulan November dengan bacaan 4634.66 J/m^2 memandangkan monsoon Timur Laut yang membawa awan tebal ke tempat kajian. Data OMUVBd telah dibezakan dengan data satelit yang lain yang bernama 'Offline Ultraviolet Product' (OUV) yang meliputi 80 tempat di seluruh semenanjung Malaysia. Keseluruhannya, persetujuan di antara data OMUVBd dan data OUV adalah baik. Perbezaan

menunjukkan purata perbezaan mutlak untuk dos eriterma ialah 24.56 J/m^2 manakala purata perbezaan relatif adalah sebanyak 0.01 J/m^2 . Ini bermakna data OMUVBd menaksir terlalu tinggi bacaan data OUV oleh kerana perbezaan data yang diguna untuk perkiraan. Untuk tempat kajian tunggal yang diambil untuk kiraan korelasi, Pulau Pinang (5.0° N , 100.0° E) dan Kuantan (3.0° N , 103.0° E) telah diambil. Keputusan menunjukkan data dari OMUVBd adalah hampir sama dengan keputusan dari OUV korelasi yang kuat iaitu $R = 0.807$ and 0.849 di kedua-dua tempat dan ini menunjukkan koefisien regresi adalah berkait. Perbezaan di dalam perkiraan ini muncul kebanyakannya kerana data input untuk liputan awan yang berbeza jenis yang digunakan dalam kedua-dua produk. Sebagai konklusi, data OMUVBd dapat diterima pakai dan pertukaran monsoon di Malaysia mempengaruhi taburan dos eriterma.

**STUDY ON SOLAR ULTRAVIOLET ERYTHEMAL DOSE DISTRIBUTION
OBTAINED BY AURA SATELLITE OVER PENINSULAR MALAYSIA.**

ABSTRACT

During the last 30 years, solar ultraviolet radiation (UV) has increased in many parts of the world mainly at mid latitude region. The information on the total of solar erythemal ultraviolet radiation incident on the earth surface is very important for the safety of human health and other living things. For this research, the data named OMUVBd retrieved from from Ozone Monitoring Instrument (OMI) that on board AURA satellite has been taken to be studied. Measurement of erythemal UV dose began in 1st January 2009 until 31st December 2009. The purposes of this study are to view the distribution of solar erythemal dose over Peninsular Malaysia using remote sensing data named OMUVBd and to differentiate this data with other satellite data. The maximum daily erythemal UV dose for Peninsular Malaysia appears in March with mean erythemal dose of 6330.78 J/m² when solar zenith angle at noon becomes zero. The average erythemal dose during the measurement period was 5447.33 J/m². The minimum erythemal dose was recorded on November with 4634.66 J/m² due to Northeast monsoon that bring a thick clouds over study area. Then OMUVBd has been compared and validates with other satellite data named Offline Ultraviolet Product (OUV) covering 80 points all over Peninsular Malaysia covering 80 points all over Peninsular Malaysia. In general, agreement between OMUVBd and OUV data is good. The difference show that the mean absolute difference for erythemal UV daily dose is 24.56 J/m² meanwhile for mean relative difference, mean bias of 0.01 J/m². These means OMUVBd overestimates the OUV

data due to the difference input data that had been used. For the single point comparison, the point near Penang (5.0° N, 100.0° E) and Kuantan (3.0° N, 103.0° E) are taken into account. The results show that the data from OMUVBd is nearly the same as the data from OUV with a strong positively correlation of $R = 0.807$ and 0.849 respectively and this shows that the coefficient of the regression was significant. The differences in measurement mostly come from different type of input data information from cloud cover information that been used in both products. As a conclusion, this OMUVBd data can be accepted and the distribution of erythemal dose was affected by several type of monsoon that occurs in Malaysia.

CHAPTER 1

INTRODUCTION

1.0 Introduction

Most of all the radiative energy entering the earth's atmosphere comes originally from the sun. The incoming solar radiation covers the entire electromagnetic spectrum from gamma and X-rays, through ultraviolet, visible, and infrared radiation to microwaves and radiowaves. The incoming solar energy may be reflected and absorbed by the Earth's surface or the atmosphere. From the solar energy that reaching the earth, 99 percent has a wavelength between 150 and 4000 nm, with nine percent in the ultraviolet ($\lambda < 400$ nm), 49 percent in the visible ($400 < \lambda < 700$ nm) and 42 percent in the infrared ($\lambda > 700$ nm) (Houghton, 1985).

1.1 Ultraviolet Radiation

UV radiation is conventionally divided into three regions (Comission Internationale de l' Eclairage, 1999 and Vanicek *et al.*, 2000; WHO, 2002) that are UVA (>315–400 nm), UVB (>280–315 nm) and UVC (>100–280 nm) as shown in Figure 1.1. UV radiation can be measured as irradiance that is the power incident per unit area and has the unit of W/m^2 or as a radiant exposure, or dose (the energy incident per unit area during a specified period of time) and the units is J/m^2 . Generally, solar erythemal ultraviolet radiation has some good and bad effects on human health and biological environments. In common, solar erythemal ultraviolet radiation is mainly controlled by the atmospheric ozone.

Stratospheric ozone absorbs completely UV-C, that extremely hazardous for us and UV-B, but UV-A was not absorbed a lot. Absence of ozone reduction can increase the UV-B radiation on earth, and it can be harmful to us (Diffey, *et al.*, 1987).

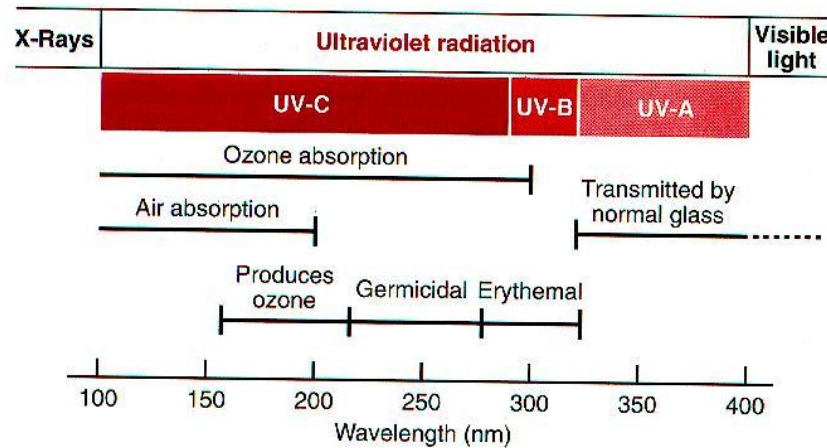


Figure 1.1: Ultraviolet (UV) region of the electromagnetic spectrum (adopted from <http://cmgm.stanford.edu/biochem201/Slides/DNA%20Repair%20-%20Doug/>)

Percentages of the energy of the incoming solar radiation is shown in Figure 1.2, of the total incoming solar radiation, 16 percent is absorbed by ozone in the stratosphere (stratospheric ozone), tropospheric water vapour and aerosols, three percent by clouds, and 51 percent by the earth's surface. The remaining 30 percent of solar radiation are backscattered by the air (six percent), reflected by clouds (20 percent) and reflected by the earth's surface (four percent) (Peixoto and Oort, 1992).

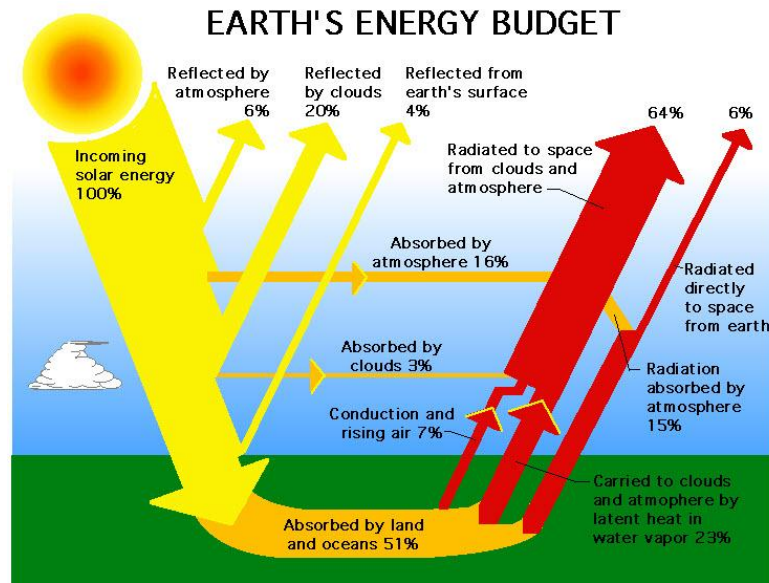


Figure 1.2: The annual mean global energy budget for the earth-atmosphere system. (adopted from http://science-edu.larc.nasa.gov/EDDOCS/radiation_facts.html)

There, about 90% of atmospheric ozone is contained in the "Ozone layer," which shields us from dangerous ultraviolet radiation from the sun (Iqbal, 1983). Stratospheric ozone is believed good for humans and other life forms because it absorbs ultraviolet UV-B radiation from the Sun. In humans, greater exposure to UV radiation can cause many cases of skin cancer, cataracts, and impaired immune systems.

Chang, *et al.* (2010) findings clearly indicate strong positive association between the skin cancer incidence rate and the annual UV exposure or the cumulative UV radiation around three or four years ago, which confirmed that their hypotheses that UV exposure can cause skin cancer and there is a latent period between the exposure and cancer diagnosis. Excessive UV exposure also can cause the damage on terrestrial plant life and aquatic ecosystems. Other UV radiation, UV-A, which is not

absorbed significantly by ozone, will causes premature aging of the skin (Fahey, 2006).

During the last 30 years, solar erythemal ultraviolet radiation has increased in many parts of the world mainly at mid latitude region. The information on the total of solar erythemal ultraviolet radiation incident on the earth surface is very important for the safety of human health and other living things. Concerns about the increase in surface UV-B have produced huge scientific and social interest, especially the discovery of the ozone hole in the Antarctic (Farman *et al.*, 1985; Solomon, 1988) and the serious ozone decreases in middle and high latitudes (WMO, 2006; Bojkov *et al.*, 1990; Mc-Peters *et al.*, 1996; Wardle *et al.*, 1997) and in result, national and international levels were doing the research and monitoring programs. Between the most important achievements of the past decade was the development of ground-based ozone and UV observation networks.

Before the 1980s, few stations conducted regular measurements, but now hundreds of ozone/UV stations are operating around the world. The data are in a good quality controlled and archived in the World Ozone and Ultraviolet Radiation Data Center of the World Meteorological Organization operated by Environment Canada (Wardle *et al.*, 1996). The most important factors influencing UV radiation at ground levels are clouds, solar zenith angle, total column ozone and surface albedo (Burrows, 1997; Kerr, 2005, Balis, *et al.*, 2007).

1.2 Factor that affecting Ultraviolet radiation

The important factors affecting the UV erythemal dose reaching the Earth's surface are described below.

i- Atmospheric ozone

Generally UV radiation is been absorbed and scattered in the atmosphere. Oxygen and ozone molecules in the upper atmosphere absorb 100% of UV-C radiation. Meanwhile for UV-B, only a few percent reach the surface of the earth because ozone molecules in the stratosphere absorbed most of it. Therefore, at the surface of the Earth the solar UV radiation is filled with a large amount of UV-A radiation and a small amount of UV-B radiation. UV-B radiation is identified to be biologically harmful; however UV-A radiation is much less damaging but is known for its ability to sun-tanned the human skin.

For instance ozone is the highest absorber of UV-B radiation the UV-B intensity at the Earth's surface depends mostly on the thickness of the ozone layer and on the total amount of ozone in the atmosphere. There is a factor that describes the relation between the sensitivity of the UV-B intensity to variations in total ozone that is being called Radiation Amplification Factor (RAF). RAF for ozone was 0.971 with solar zenith angle. (Lee, J et al, 2012)

ii- Solar elevation

The angle between the horizon and the direction to the sun is called solar elevation meanwhile the angle between the zenith and the direction to the sun is called solar zenith angle (SZA) and it is often used in place of the solar elevation. For high solar

elevations the rays from the sun have a shorter path through the atmosphere and cause UV radiation become more intense because it went through a smaller quantity of absorbers. Therefore the UV irradiance depends strongly on the solar elevation it varies with latitude, season and time, being maximum in the tropics, in summer and at noon.

iii- Altitude

The UV irradiance increases with altitude because the quantity of absorbers in the overlapping atmosphere decreases with altitude. Measurements show that the UV irradiance increases by six to eight percent per 1000 m increase in altitude (Zaratti *et al.*, 2003).

iv- Aerosol

Regarding the aerosols its effect is more complex due to its great geographical and temporal variation, among its variety material composition. For example, the scattering of volcanic aerosol reduces about five percents to the Erythemal UV irradiance (Tsitais and Yung, 1996) and the largest reductions in UV are more than 50% associated with smoke and dust clouds in Africa and South America (Herman *et al.*, 1999).

v- Clouds and haze

The UV irradiance is increase when the sky is cloudless. Clouds commonly reduce the UV irradiance but the attenuation by clouds depends on both type of clouds (optical depth of clouds) and the thickness. Thin or scattered clouds have only a little effect on UV at the ground compared with thick cloud. In hazy conditions, the

existence of water vapour and aerosols on water vapour may cause UV radiation to be absorbed and scattered and this leads to decreasing of the UV irradiance. Study shows that cloudiness often affects the influence of ozone changes on UV radiation and may reduce, cancel or enhance the expected UV signal (Glandorf *et al.*, 2005).

vi- Ground reflection

Part of the UV radiation that hit the ground is absorbed by the Earth's surface and part of it is reflected back to space. The properties of the surface will affect the quantity of reflected radiation. For most natural surfaces such as grass, soil and water reflect less than about 10% of the incoming UV radiation. Fresh snow may reflect up to about 80% of the incident UV radiation. Sand can reflect about 25% of the UV radiation and these can increase the UV exposure at the beach. About 95% of the UV radiation penetrates into the water and 50% penetrate to a depth of about three meter. Snow depth and snow quantity are the most significant factors influencing surface albedo in the UV range and the relationship has been well studied (Blumthaler and Ambach, 1988; McKenzie *et al.*, 1998; Weihs *et al.*, 1999, 2001; Schmucki and Philipona, 2002).

Figure 1.3 estimates show that erythemal radiation at Earth's surface, mostly at midlatitudes in both hemispheres (bottom panel) has increased at most part of the world over the period 1979 to 2008. The increases in the Southern Hemisphere would have been larger without the offsetting changes due to clouds and aerosols (upper panel). The smallest estimated changes in erythemal radiation are in the tropics because observed total ozone changes over this period are smallest there. The

shaded areas surrounding the figure lines represent the uncertainties in the estimated changes (Fahey, 2006).

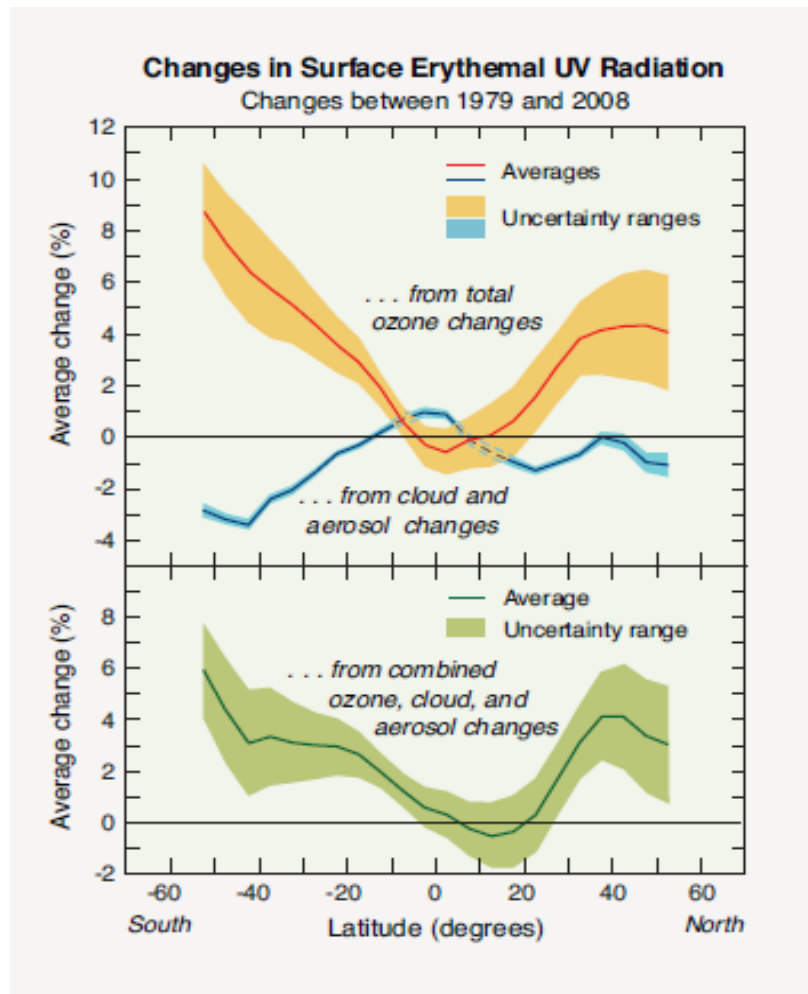


Figure 1.3: Long-term changes in surface erythemal radiation (Fahey, 20 Questions: 2010 Update)

The UV-B radiation (about 0.5% of the solar radiation) is the cause for most of the effects of sunlight on the body. It is the main source of sunburn and tanning, other than the construction of vitamin D3 in the skin, and it also had influences the immune system. UV-B radiation does not penetrate far into the body; most of it is absorbed in the superficial tissue layers in about of 0.1 mm depth. However, primary reactions in the superficial layers have significances throughout the body (van der Leun and Gruijl, 1993).

In general, sunburn can be avoided by sensible behaviour. The skin needs to adapt from its winter condition to the increased UV-B irradiance in summer. The prevention of sunburn depends on going through this process carefully. In overall, it has been accepted that the UV-B portion produces the more deleterious biological effects but the UV-A radiation has been shown to produce the same biological effects, most likely through alternative mechanisms (Treina *et al.*, 1996).

1.3 UV index

The erythemal UV index as known as the UV index (UVI) is a valuation of the UV levels that are important for its effects on the human skin, where one unit equals 25 mW/m². It is usually specified for local solar noon, when the Sun is highest in the sky, and it is valid for clear-sky conditions so that effects of clouds shielding part of the UV radiation are not taken into account.

The erythemal UV index is a calculated quantity derived from the erythemal irradiance, which is a combination of the UV irradiance at the ground weighted by the CIE spectral action function. The CIE action spectrum is a model for the susceptibility of the caucasian skin to sunburn (erythema). It is recommended by McKinlay & Diffey (1987) and adopted as a standard by the Commission Internationale de l'Éclairage (International Commission on Illumination). Of the global UV radiation at the ground, 94% is UV-A, 6% is UV-B meanwhile the erythemal UV irradiance, however, 17% is UV-A, 83% is UV-B.

1.4 Daily Ultraviolet Erythemal Dose

The integration takes the cloud cover into account and thus leads to an estimate of the daily erythemal UV dose. The total amount of UV radiation absorbed by the human skin during the day, expressed in kJ/m^2 . M. van Weele and van der A, (2006) calculate the solar UV Erythemal dose using data from SCIAMACHY data archive. The cloud covers data information is available once every hour from METEOSAT, one of the geostationary satellites in order to compute the UV dose of the previous day.

Clear-sky UV dose or maximum UV dose can be determined by the absence of clouds. In Figure 1.4, the UV dose is compute in time steps of 10 minutes and these values are summed to acquire the total erythemal UV dose for the day. The blue curve shows the UV dose in intervals of 10 minutes for De Bilt (Netherlands) with the value at the left y-axis. The measurement is on 1 June 2002 with a completely cloud-free day condition. The red curve shows the cumulative UV dose, with as end value 4.0 kJ/m^2 on the right y-axis.

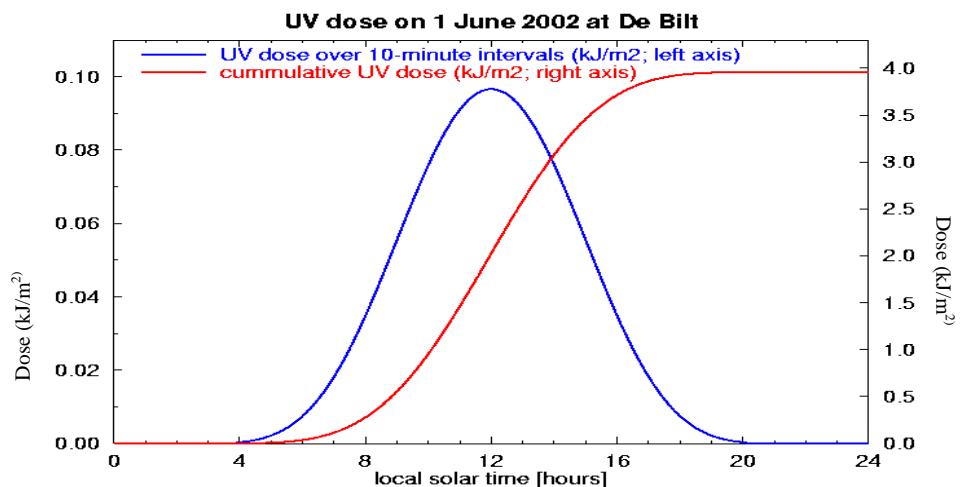


Figure 1.4: UV dose in De Bilt on 1 June 2002 (Jos van Geffen & Ronald van der A, 2007)

Figure 1.5 shows the UV dose in intervals of 10 minutes for Augsburg (Germany) on 1 June 2002, showing the effect of clouds passing over the area. The green curve is the clear-sky UV dose, by assuming there are no clouds, while the red curve is the actual UV dose. The blue curve shows the cloud cover fraction, which is given in one-hour intervals. The clear-sky UV dose for the full day is 4.4 kJ/m^2 but the actual erythemal UV dose for the full day is 3.7 kJ/m^2 .

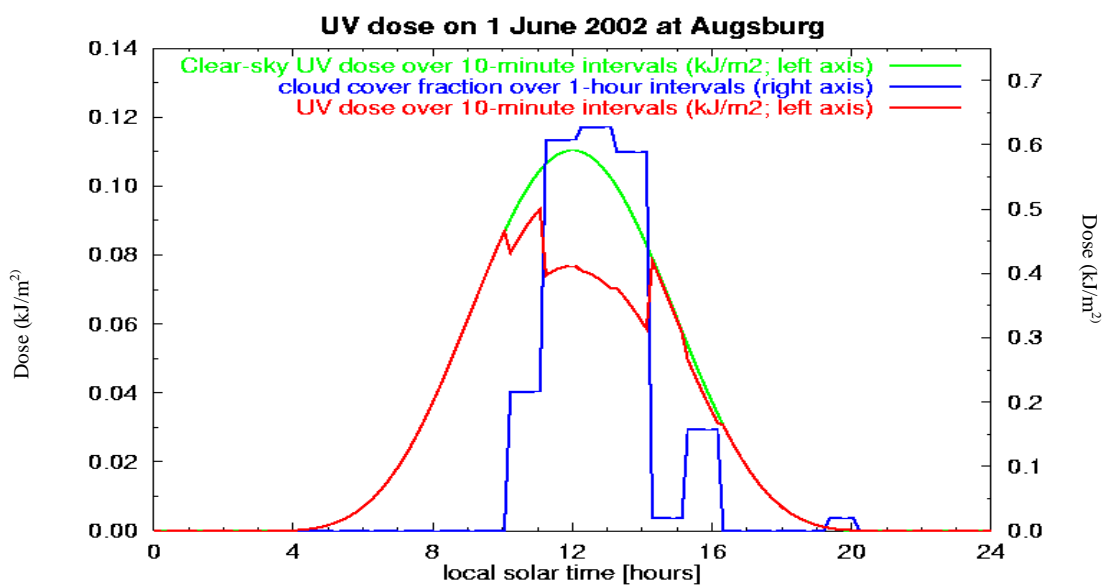


Figure 1.5: UV dose in Augsburg on 1 June 2002 (Jos van Geffen & Ronald van der A, 2007)

1.5 Problem Statement

Despite the lack of study on Ultraviolet erythemal dose in Malaysia, there is also lack of data available for ground-based data measurement for UV radiation. Furthermore, the studies using satellite data was rarely considered for equatorial region. They provide in situ ground-truth values, are easily calibrated and recalibrated, have a finer spatial and temporal resolution, etc.

Notwithstanding, ground-based observation alone is insufficient to address the global ozone/UV problems for its inherent limitations, which include sparse and non-uniform spatial coverage, variable observation standard and quality, and short observation periods for the majority of stations. A combination of ground-based and space-borne UV observation would be ideal to best characterize the spatial and temporal variability of UV.

The above limitations can be overcome or lessened by means of space-borne remote sensing. In contrast to ground observation, satellite provides global complete coverage at a moderate resolution with standard sensors. So far, UV has been observed from space for more than 20 years. Early satellite UV measurements were made by the Backscatter Ultraviolet (BUV) sensor onboard the Nimbus 4, which was launched in 1970 and continued functioning for several years (Stolarski *et al.*, 1997).

1.6 Objectives of the Study

The objectives of the study are summarized as follows:

- 1- To study the ultraviolet erythemal dose obtained from OMUVBd satellite data.
- 2- To study the distribution of ultraviolet erythemal dose over peninsular Malaysia on 2009
- 3- To compare erythemal dose between two satellite data that are OMUVBd from AURA satellite and OUV O3M SAF from GOME-2 satellite.

1.6 Outline of the Thesis

This thesis contains 5 chapters, which are described in brief as follows:

Chapter 1 provides an overview of this study. Additionally, this chapter presents a brief background about ultraviolet radiation and the factors that affect it reaching the surface. Furthermore, a statement of problem and the objectives of this study are also presented in chapter 1. Chapter 2 includes a definition and brief background about OMI and OMUVBd, and the other satellite data that is OUV O3M SAF data also has been presented in this chapter along with literature review of the validation of OMUVB.

Chapter 3 gives the detailed in OMUVBd and OUV data and it describe the sources of the data and the software used. Study area and period also has been presented in this chapter. Meanwhile in chapter 4, the data analysis and discussion of all the obtained result is presented here. 12 months map and a graph of daily distribution of UV daily dose has been discussed.

In chapter 5, the comparison is done between OMUVBd and OUV data and the difference between both data is been discussed in detail and the conclusion is presented in chapter 6.

CHAPTER 2

LITERATURE REVIEW

2.0 Introduction

In contrast to ground observations, satellites provide complete global coverage at a moderate resolution with standardized sensors. UV has been observed from space for more than 30 years. Early satellite UV measurements of the backscatter ultraviolet (BUV) sensor were made by the Nimbus 4 that was launched in 1970 and functioned for quite a few years. Nimbus 7 provided the longest high-quality UV space-borne observation from 1978 to 1993 with TOMS. This dataset can be used for monitoring long-term trends in total column ozone, and investigating seasonal chemical depletions in ozone occurring in both the southern and northern hemisphere polar springs (Kalliskota *et al.*, 2000; Kaurola *et al.*, 2000; Pubu and Li, 2001).

2.1 AURA Satellite

AURA is one of the NASA's long-term Earth Observing System (EOS) mission and it was launched July 15, 2004, from Vandenberg Air Force base in California. The AURA spacecraft was launched into a near polar, sun-synchronous orbit with a period of around 100 minutes. Every 16 days the spacecraft repeats its ground track to provide atmospheric measurements over virtually every point on the Earth in a repeatable pattern, permitting assessment of atmospheric phenomena changes in the same geographic locations throughout the life of the mission.

The AURA spacecraft is planned for a six-year lifetime. The spacecraft orbits at 705 km with a 1:45 PM \pm 15 minute equator crossing time and in a sun-synchronous orbit (98° inclination). AURA limb instruments are all designed to observe roughly along the orbit plane. The AURA spacecraft carries four instruments: the Microwave Limb

Sounder (MLS), the High Resolution Dynamics Limb Sounder (HIRDLS), Tropospheric Emission Spectrometer (TES) and Ozone Monitoring Instrument (OMI). MLS is on the front of the spacecraft (the forward velocity direction) while HIRDLS, TES and OMI are mounted on the nadir side.

EOS AURA's Instruments, HIRDLS, MLS, OMI, and TES contain advanced technologies that have been developed for use on environmental satellites. Each instrument provides unique and complementary capabilities that will enable daily global observations of Earth's atmospheric ozone layer, air quality, and key climate parameters.

2.1.1 Ozone Monitoring Instrument

OMI was constructed by Dutch Space and TNO TPD in The Netherlands with collaboration with Finnish VTT and Patria Advanced Solutions Ltd. The Royal Netherlands Meteorological Institute (KNMI) is the Principal Investigator Institute. Overall responsibility for the OMI mission lies with The Netherlands Agency for Aerospace Programmes (NIVR) with the participation of the Finnish Meteorological Institute (FMI). As shown in Figure 2.1, Ozone Monitoring Instrument (OMI) is a nadir viewing spectrometer that designed to monitor ozone and other atmospheric components (Levelt *et al.*, 2006). OMI covers the wavelength range from 264 to 504 nm.

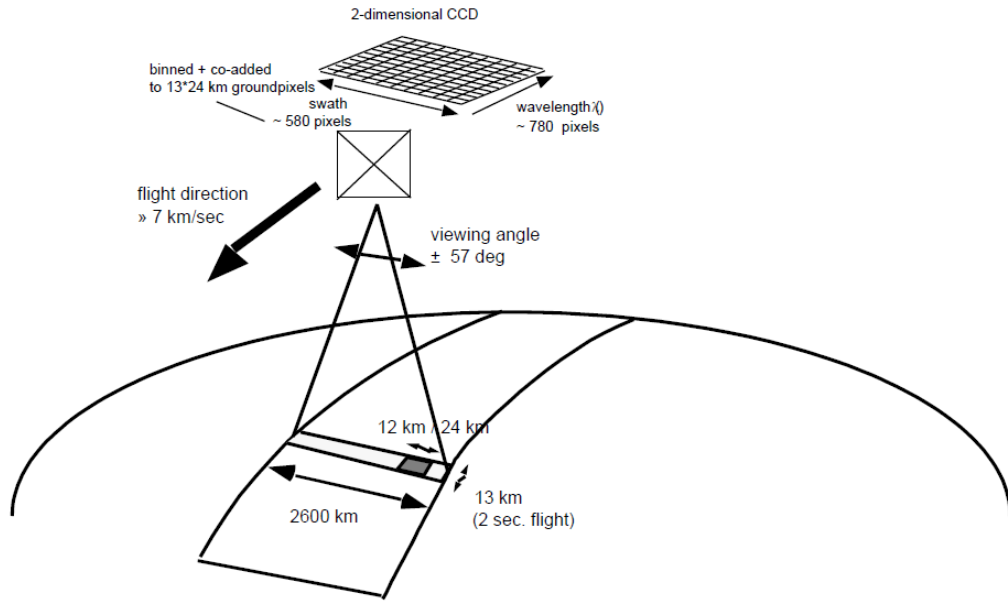


Figure 2.1: Measurement design of Ozone Monitoring Instrument (OMI User Guide, 2009)

The OMI surface UV algorithm first estimates the clear-sky surface irradiance using the total column ozone measured by OMI, elevation, climatological surface albedo, solar zenith angle, and latitude-dependent climatological ozone and temperature profiles. Next, the clear-sky irradiance is reproduced by multiplied the clear-sky surface irradiance to a factor that accounts for the attenuation of UV radiation by clouds and non-absorbing aerosols. The characteristic of the instrument is described in Table 2.1

Table 2.1 OMI instrument characteristic (OMI User Guide, 2009)

Item	Parameter
Visible:	350 - 500 nm
UV:	UV-1, 270 to 314 nm, UV-2 306 to 380 nm
Spectral resolution:	1.0 - 0.45 nm FWHM
Spectral sampling:	2-3 for FWHM
Telescope FOV:	114 (2600 km on ground)
Ifov:	3 km, binned to 13 x 24 km
Detector:	CCD: 780 x 576 (spectral x spatial) pixels
Mass:	65 kg
Duty cycle:	60 minutes on daylight side
Power:	66 watts
Data rate:	0.8 Mbps (average)

2.1.2 UV algorithm overview

Figure 2.1 shows the overview of the OMI algorithm. The amount of ultraviolet radiation in the UVA (320 nm – 400 nm) and UVB (290 nm-320 nm) spectral ranges that reach the surface of the Earth is calculated by Rayleigh scattering from the molecular atmosphere, the absorption of ozone, scattering by clouds, both scattering and absorption by aerosols and from the surface reflection. The algorithm is based on corrections to calculated clear-sky UV irradiance, E_{Clear} . The calculation procedure is determined on table lookup and either cloud/non-absorbing aerosol correction or absorbing aerosol correction. The type of correction is selected based on the two threshold values of the aerosol index (AI) (calculated from 331 nm and 360 nm radiances) and Lambertian Equivalent Reflectivity (LER) (360 nm) as described below. The surface albedo and snow effects are estimated using the TOMS monthly minimum Lambertian Effective surface Reflectivity (MLER) global database (Herman and Celarier, 1997).

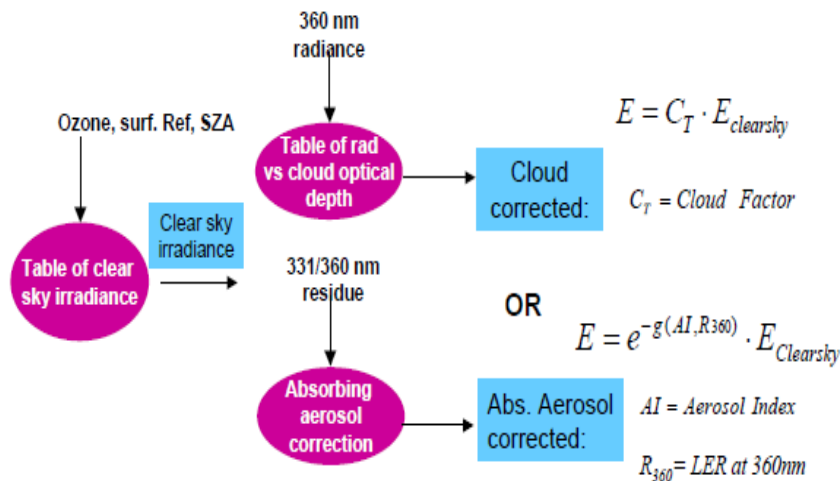


Figure 2.2: OMI UV algorithm overview (Levelt, 2006)

The current algorithm (Krotkov *et al.*, 1998, 2001, 2002) does not account for absorbing aerosols (e.g. organic carbon, smoke, and dust) or trace gases (e.g., NO₂, SO₂), which are known to lead to systematic overestimation of the surface UV irradiance (Chubarova, 2004; Arola *et al.*, 2009) and the cirrus effect on UV radiation is neglected. The OMI derived surface UV irradiances are predictable to show overestimation for regions that are affected by absorbing aerosols.

For local solar noon, the UV irradiances are calculated once a day. Corrections are not made for possible variations in cloudiness or total column ozone between the local noon and satellite overpass time. The OMUVBd (version 3) data products selected are TOMS-like daily Level three (L3) gridded (lat-lon 1°×1°) data product.

2.2 O3M SAF

Satellite Application Facility on Ozone and Atmospheric Chemistry Monitoring (O3M SAF) of the Satellite Application Facility on Ozone and Atmospheric Chemistry Monitoring Service Specification (EUMETSAT) Joint effort of ten institutes in seven European countries, FMI is the leading entity Part of EUMETSAT's Polar System (EPS) ground segment. Three Metop satellites are used to cover some 15 years up to 2020. METOP-A was successfully launched 19 October 2006 Ozone, trace gases and aerosols from GOME-2.

2.2.1 Offline UV daily dose.

Offline surface UV (OUV) products contain the most important parameters of the solar radiation that can be harmful to life and materials on the Earth. These quantities include daily doses and maximum dose rates of integrated UV-B and UV-A radiation together with values obtained by different biological weighting functions, solar noon

UV index and quality control flags. The offline means products are available to users in two weeks from sensing. Table 2.2 show the O3M SAF Product for Offline UV Daily Dose.

For theoretical basis the OUV products are derived from O3M SAF near real-time total ozone column product (NTO/O3) and Advanced Very High Resolution Radiometer (AVHRR) reflectances, then combining data from two different instruments on board the Metop-A satellite. Sampling of the diurnal cloud cycle is enhanced by using additional AVHRR data from the NOAA satellites, available through the data exchange between EUMETSAT and NOAA.

Table 2.2 O3M SAF Product Tables for Offline UV daily Dose (Jari Hovila *et al.*,2011)

O3M-17	Offline UV daily dose, erythemal (CIE) weighting		OUV/DD_CIE
Type	Product		
Applications and users	Climate monitoring		
Characteristics and methods	Radiative transfer modeling		
Comments			
Generation frequency	1 per day		
Input satellite data	GOME-2 via NTO, HIRS/4 via HTO, and AVHRR (MetOp/NOAA)		
Dissemination			
Format	Means	Type	
HDF5	FTP, DVD	Offline	
Accuracy			
Threshold	Target	Optimal	
50%	20%	10%	
Verification method	Comparison with ground-based measurements		
Coverage, resolution and timeliness			
Spatial coverage	Spatial resolution	Timeliness	
Global	0.5° x 0.5°	2 weeks	

The process of the product was take part at the Finnish Meteorological Institute's (FMI). OUV processor reads the look-up tables containing the radiative transfer

results, calculated using the VLIDORT model. Then the files containing the extraterrestrial solar irradiance and list of the validation sites are read. Then the values of the biological weighting functions at the wavelengths of the extraterrestrial solar irradiance spectrum are calculated. OUV product is validated by FMI. The validation is based on detailed comparison of existing satellite data with ground-based measurements. OUV product quality is constantly monitored by FMI. The online monitoring is based on a tracking value calculated from the daily product.

The O3M SAF offline surface UV product is derived from the measurements of the operative polar orbiting METOP and NOAA satellites. The product contains the most important quantities of the Sun's radiation that can be harmful to life and materials on the Earth. These quantities include daily doses and maximum dose rates of integrated UV-B and UV-A radiation together with values obtained by different biological weighting functions, solar noon UV index and quality control flags. The product is calculated in a 0.5 degree regular grid and stored in a HDF5 file (Arola *et al.*, 2009). These data were generated under the auspices of the O3M SAF project of the EUMETSAT

The O3M SAF offline surface ultraviolet product is being used to do the comparison with OMUVBd and the result is discussed in detail in chapter 5.

2.3 Validation on OMI Data

A first validation of OMI UV retrievals is given by Tanskanen *et al.* (2007): they compared the surface UV radiation data from OMI with those derived from 18 ground-based stations located at different sites in Europe, Canada, Japan, USA and Antarctic. The validation results showed that OMI data are in general suitable to

monitor solar UV radiation levels but it was noticed a positive bias of the satellite derived UV in urban sites, due to the effect of pollution. For flat, snow-free regions with modest loadings of absorbing aerosols or trace gases, the OMI derived daily erythemal doses have a median overestimation of 0–10 %, and some 60 to 80% of the doses are within $\pm 20\%$ from the ground reference. For sites that mostly affected by absorbing aerosols or trace gases one expects, bigger positive bias up to 50% is being observed. For high-latitude sites the satellite-derived doses are occasionally underestimated by up to 50% because of unrealistically small climatological surface albedo.

Intercomparisons were also studied in two French sites: Villeneuve d'Ascq and Briançon (Buchard *et al.*, 2008). Comparisons of the erythemal dose rates and erythemal daily doses at Villeneuve d'Ascq show that OMI overestimates surface UV doses at by about 13% for clear sky and that on all sky conditions, the bias slightly increases. Meanwhile at Briançon, a bias is observed if data corresponding to snow-covered surface are excluded.

The other comparison was held at Thessaloniki, Greece from September 2004 to December 2007 on spectral ultraviolet overpass irradiances from the Ozone Monitoring Instruments (OMI) against ground-based Brewer measurements at. It is demonstrated that OMI overestimates UV irradiances by 30%, 17% and 13% for 305 nm, 324 nm, and 380 nm respectively and 20% for erythemally weighted irradiance. The bias between OMI and Brewer increases with increasing aerosol absorption optical thickness (Kazadzis *et al.*, 2009).

Weihls *et al.* (2008) result shows the average difference between OMI and ground-based data at five stations. OMI are on average higher by 25% at the station Grossenzersdorf, 27% at University of Veterinary Medicine, 32% at Bad Voeslau, 24% at the station TGM, 30% at BOKU and 37% at station Strebersdorf. The median of the differences of OMI to ground UV stations is with values between 12 and 26% lower since it does not include outliers.

The erythemally weighted UV dose rates at local noon and the daily doses estimated from OMI were plotted against those measured from the Brewer spectrometer at Reading. The result show that the OMI data overestimated the surface irradiance which may result from the effects of the tropospheric aerosol absorption, the cloud optical thickness (and assumption of constant cloud all day) and the satellite solar zenith angles.

Ialongo *et al.* (2008) study found that OMI data overestimate ground-based erythemally weighted data compared with two spectrometer, that are Brewer and YES Radiometer (biases about 20%), probably because of the effect of absorbing aerosols in an urban site such as Rome.

In Buntoung *et al.* (2010) the UV index retrieved from OMI observations and measured from broadband instruments at four sites in Thailand were compared. The comparisons show a positive bias for the OMI data with respect to the ground-based measurements. The differences between the two data sets were 30–60% for all data and were 10–40% for cloudless data. The differences for the cleanest site showed better agreement than those for the more urban sites.

CHAPTER 3

METHODOLOGY AND DATA FORMAT

3.0 Introduction

The data formats, study area, period of study and image processing methods have been discussed in detail and significant. In this chapter, the image processing software was described, in order to analyze the data after process will be given too. The methods and the techniques used to obtain the output for research purpose will also discussed in detail.

3.1 Remote Sensing Data Format

Remote sensing for monitoring of the earth requires a variety of diverse platforms and instruments, ranging from hand-held close range spectrometers to image and sounders on board satellites many thousand kilometers from earth. The diverse types of sensor data have different disadvantages and strengths. Different types of sensors are suitable for the purposes of different studies.

As mentioned in Chapter 2, the AURA satellite was design with advanced technologies that have been developed for use on environmental studies. Ozone Monitoring Instrument (OMI) that on board of the AURA satellite provides unique and complementary capabilities that will enable daily global observations of Earth's atmospheric ozone layer, air quality, and key climate parameters.